N70-25702

NASA TECHNICAL MEMORANDUM

NASA TM X-2009

NASA TM X-2009

CASE FILE COPY

MEASUREMENTS OF FLUCTUATING PRESSURES IN 8- BY 6-FOOT SUPERSONIC WIND TUNNEL FOR MACH NUMBER RANGE OF 0.56 TO 2.07

by Raymond J. Karabinus and Bobby W. Sanders

Lewis Research Center
Cleveland, Ohio 44135

NATIONAL AERONAUTICS AND SPACE ADMINISTRATION • WASHINGTON, D. C. • MAY 1970

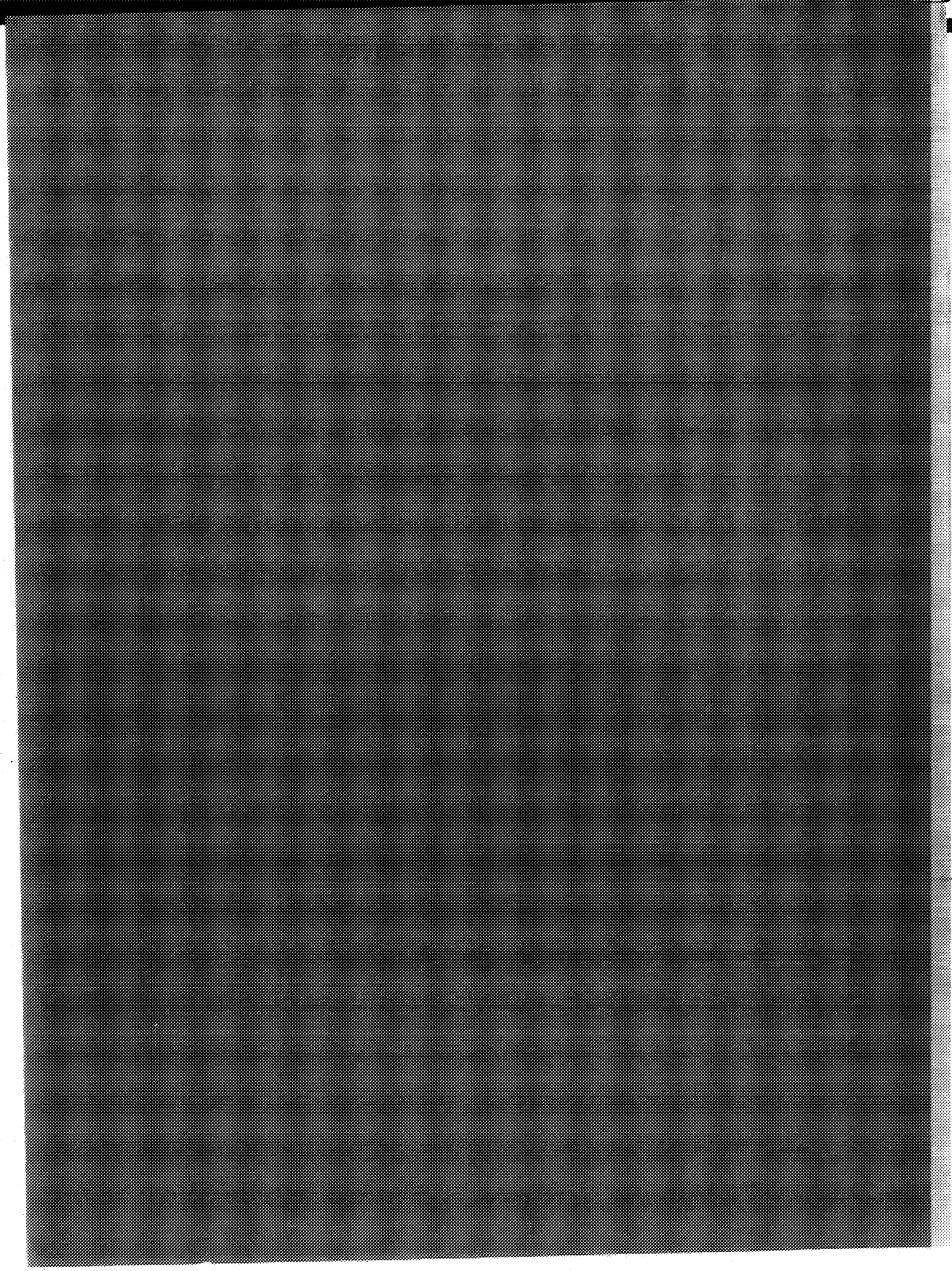

1. Report No. NASA TM X-2009	2. Government Accession No.	3. Recipient's Catalog No.
4. Title and Subtitle MEASUREMENTS OF FLUCTUATING PRESSURES IN 8- BY 6-FOOT SUPERSONIC WIND TUNNEL FOR MACH NUMBER RANGE OF 0.56 TO 2.07		5. Report Date May 1970 6. Performing Organization Code
7. Author(s) Raymond J. Karabinus and Bobby W. Sanders		8. Performing Organization Report No. E-5518
9. Performing Organization Name and Address Lewis Research Center National Aeronautics and Space Administration Cleveland, Ohio 44135		10. Work Unit No. 720-03 11. Contract or Grant No. 13. Type of Report and Period Covered Technical Memorandum
12. Sponsoring Agency Name and Address National Aeronautics and Space Administration Washington, D.C. 20546		14. Sponsoring Agency Code
15. Supplementary Notes		

16. Abstract

An investigation was conducted on the pressure perturbations in the bellmouth, test section, and diffuser of the tunnel. The principal disturbance in the test section occurred near Mach 0.75 at a frequency of about 500 Hz and appeared to be a flow resonance within the porous region of the test section. Disturbances at 800 Hz originated from the compressor, and the other higher frequency disturbances appeared to be generated by the holes in the test section walls.

17. Key Words (Suggested by Author(s))	18. Distribution Statement
Wind tunnel, transonic Fluctuating pressures Porous test section Tunnel noise background	Unclassified - unlimited

19. Security Classif. (of this report)	20. Security Classif. (of this page)	21. No. of Pages	22. Price*
Unclassified	Unclassified	32	$3.00

*For sale by the Clearinghouse for Federal Scientific and Technical Information
Springfield, Virginia 22151

MEASUREMENTS OF FLUCTUATING PRESSURES IN 8- BY 6-FOOT SUPERSONIC WIND TUNNEL FOR MACH NUMBER RANGE OF 0.56 TO 2.07

by Raymond J. Karabinus and Bobby W. Sanders

Lewis Research Center

SUMMARY

Pressure perturbations have been observed to exist in the flow field of the Lewis 8- by 6-foot supersonic wind tunnel. Therefore, dynamic pressure measurements were made with flush-mounted transducers located in the bellmouth, in the test section, in the tunnel diffuser, and on a cone-cylinder model mounted in the test section. The principal disturbance in the test section occurred near Mach 0.75 at a frequency of about 500 hertz, and a secondary disturbance existed at 800 hertz. At supersonic speeds, there were less prominent disturbances at several frequencies from 800 to 8000 hertz. The disturbance at 800 hertz originated from the compressor, and the 500-hertz disturbance appeared to be a flow resonance within the porous region of the test section. The predominant high-frequency preturbations above 2000 hertz appeared to be generated by the holes in the test section wall. The pressure oscillations in the subsonic diffuser did not appear to influence the test section perturbations.

INTRODUCTION

Several investigations of the fluctuating pressures on the surface of models in the Lewis 8- by 6-foot supersonic wind tunnel have indicated background noise in the high subsonic speed range (e.g., ref. 1). Even though this type of pressure disturbance has been observed in other transonic wind tunnels (refs. 2 to 5), the mechanism of these pressure disturbances is not fully understood. Further information on the nature of these disturbances was obtained by measuring the frequencies and amplitudes of the disturbances in the 8- by 6-foot supersonic wind tunnel at Mach numbers from 0.56 to 2.07 with average test section porosities of 6.2, 3.1, and 0 percent. The pressure fluctuations were measured with flush-mounted transducers in the bellmouth, in the test section, in the diffuser, and on a cone-cylinder model in the test section.

SYMBOLS

ΔC_p	fluctuating pressure coefficient, $\Delta p/q$
K	pressure transducer
M	Mach number
P	total pressure
p	static pressure
Δp	fluctuating pressure
q	dynamic pressure
Re	Reynolds number
φ	power spectral density

Subscripts:

Aft	aft end of test section
Bal	balance chamber
E	diffuser exit
p-p	peak to peak
rms	root mean square
0	free stream

TUNNEL TEST SECTION AND MODEL

The Lewis 8- by 6-foot supersonic wind tunnel is a continuous-operation return-flow wind tunnel with a Mach number range of 0.4 to 2.07. The test section leg of the tunnel is shown in figure 1. The tunnel return leg contains cooling coils and an air dryer building. The axial flow compressor, which is driven by a 87 000-horsepower electric drive system, has a maximum airflow capacity of 2 million cubic feet per minute (56 000 m^3/min) and a maximum pressure ratio of 1.8. The compressor discharge air passes through a honeycomb and screen before entering the bellmouth of the flexible nozzle. The contour of the flexible nozzle walls is variable during tunnel operation and controls the test section supersonic Mach number. A variable second throat at the downstream end of the test section is used to control the subsonic Mach number in the test section. This second throat consists of two hinged doors that are swung into the flow to restrict the flow area.

The test section is 8 feet (2.438 m) high, 6 feet (1.829 m) wide, and 23.5 feet (7.163 m) long. The aft 8 feet (2.438 m) of the test section is perforated with 1.00-inch-(25.4-mm-) diameter holes inclined forward at 60°. While the design objective was to have uniform perforations giving a porosity of 6.0 percent over the entire length, the existing support structure limited hole placement so that some local regions of the wall were unperforated. As a result, the average porosity was 6.2 percent, and the local porosity in a uniformly perforated region (illustrated in fig. 2) was 11.2 percent. A calibration test reported in reference 6 indicated that the optimum average porosity for small models was 3.1 percent. This lower porosity was obtained by plugging alternate holes. Results are presented in this report for both porosities and the nonporous test section that was obtained by plugging all the holes.

The cone-cylinder model details are shown in figure 3, and its location in the porous test section is shown in figure 4. This model produced a blockage of 0.284 percent.

Tunnel parameters such as Reynolds number, total pressure, static pressure, dynamic pressure, tunnel pressure ratio, and suction airflow are presented in figure 5. The optimum pressure ratios required for subsonic flow are p_{Bal}/P_0 (fig. 5(e)), which is controlled by the second throat, and p_{Aft}/p_{Bal} (fig. 5(f)), which is controlled by varying balance chamber pressure. For optimum supersonic flow, the Mach number is controlled by the flexible wall and the p_{Bal}/P_0 by varying the balance chamber pressure.

INSTRUMENTATION

Miniature quartz pressure transducers, numbered K1 to K6, were flush-mounted in the bellmouth, on the test section wall, on a cone-cylinder model in the test section, and in the diffuser of the tunnel, as indicated in figure 4. A schematic diagram of the data measuring equipment is shown in figure 6. The system had an overall frequency response from 1 to 10 000 hertz. The pressure transducer outputs were recorded on magnetic tape by an FM record-reproduce system and then replayed to obtain the data readouts.

Direct-writing oscillograph traces were scaled for the fluctuating peak-to-peak pressure amplitudes Δp_{p-p} and the fluctuating rms pressure values Δp_{rms} were obtained from a true rms voltmeter and were recorded on the oscillograph traces.

Spectral displays were obtained by replaying the magnetic tape into a sonic spectrum analyzer that produced instantaneous rms pressure displays from 40 to 20 000 hertz with a variable bandwidth of five times the square root of the frequency. The power spectral density displays were obtained from 2-second-duration tape loops that were

replayed through a wave analyzer system. For the displays presented in this report, the frequency bandwidth was 10.8 hertz with a low-pass filter of 2100 hertz.

RESULTS AND DISCUSSION

The fluctuating pressure data for each of the transducers are presented in two figures. The first figure shows the fluctuating peak-to-peak pressure coefficient $\Delta C_{p_{p-p}}$ and the fluctuating root-mean-square pressure coefficient $\Delta C_{p_{rms}}$ levels for the range of Mach numbers from 0.56 to 2.07. In the second figure, for each of the transducers, spectral displays of the instantaneous $C_{p_{rms}}$ amplitude are presented for the 6.2-, 3.1-, and 0-percent-average-porosity test sections. These displays are shown for selected Mach numbers that either illustrate trends or are representative of a range of Mach numbers.

Fluctuating pressure data for transducer K4, which was located near the center of the perforated wall, are presented in figure 7. The figure shows that a sharp peak in amplitude occurred at high subsonic speeds with the 3.1-percent-porosity test section. The maximum peak-to-peak fluctuating pressure level of 39 percent of dynamic pressure and the maximum rms level of 6.3 percent of dynamic pressure occurred at Mach 0.75. At this speed, the rms level for the 3.1-percent-porosity test section is approximately $2\frac{1}{2}$ times the rms value obtained at the other Mach numbers. Changing the test section average porosity to 6.2 or to 0 percent eliminated this sharp peak at subsonic speeds. At other Mach numbers, the 3.1- and 6.2-percent porosities produced similar results, but the 0-porosity produced the lowest amplitudes at speeds above Mach 0.8. The spectral displays in figure 8 for the 3.1-percent-porosity configuration show that, at Mach 0.75 and 0.80 (figs. 8(a) and (b), respectively), the main disturbance occurred near 500 hertz and that a secondary disturbance was prominent at 800 hertz. Lesser disturbances also existed at several other frequencies. At Mach 0.91 (fig. 8(c)), the 500-hertz disturbance disappeared, but the 800- and 1800-hertz disturbances remained at about the same amplitudes as at lower speeds. At Mach 1.76 (fig. 8(d)), the disturbances were of relatively low amplitude. For the nonporous test section at Mach 0.75 (fig. 8(e)), there again were prominent peaks at 500 and 800 hertz, but the 500-hertz amplitude was less than that with 3.1-percent porosity. Increasing the porosity to 6.2 percent (fig. 8(f)) essentially eliminated the 500-hertz disturbance, but the 800-hertz peak became more prominent than it was at any other test condition.

Transducer K3, which was located at the beginning of the perforations, showed a similar peak in amplitude at the high subsonic speeds (fig. 9) with the 3.1-percent-porosity test section. However, near Mach 0.8, the highest amplitude was about one-

third less than it was at the transducer K4 location. This peak again was eliminated by changing the porosity to either 6.2 or 0 percent. At subsonic speeds, the 6.2- and 0-porosity results were similar to those for K4. For supersonic Mach numbers, the activity with 6.2-percent porosity was generally greater than that with 3.1-percent porosity. In either case, the activity was again greater than it was for the nonporous test section at speeds above Mach 0.8. The spectral displays for the subsonic Mach numbers are shown in figures 10(a) to (c) to be similar to those for the K4 transducer. However, for Mach 1.76 (fig. 10(d)), pressure peaks near 2500 and 5000 hertz have increased substantially. With 0-percent porosity (fig. 10(e)), the results were similar to those for K4, but with 6.2-percent porosity (fig. 10(f)), the 800-hertz disturbance was much less.

Fluctuating pressure magnitudes recorded for transducer K2, which was located farther upstream in the solid portion of the test section, are presented in figure 11. At this particular transducer location, the fluctuating pressure levels for all three test section porosities were of about the same magnitude except near Mach 0.8, where the 3.1-percent-porosity test section was only slightly greater. The spectral displays show that at Mach 0.75 and 0.80 (figs. 12(a) and (b), respectively) the results were similar to those for the K3 transducer with large disturbances at 500 and 800 hertz. At Mach 0.90 (fig. 12(c)), the 800-hertz disturbance was somewhat less than that at K3, but at all other frequencies the disturbances were substantially reduced. At supersonic speeds (fig. 12(d)), only the 2000-hertz frequency was prominent, and the amplitudes at all frequencies were less. With 0-percent porosity at Mach 0.79 (fig. 12(e)), the general activity was similar to that with 3.1-percent porosity, with the exception that a peak at 200 hertz became evident. With 6.2-percent porosity (fig. 12(f)), the 800-hertz peak was most prominent.

For transducer K1, which was located in the bellmouth (fig. 13), the results were essentially unchanged when the test section porosity was varied. The spectral displays in figure 14 show that a resonance occurred at 800 hertz for all test conditions, but the 500-hertz disturbance did not exist. The 800-hertz disturbance is attributed to the compressor blades since it corresponds to the rotor revolutions per second times the number of blades in the last stage. Since the disturbance at 500 hertz decreases from a maximum in the test section to practically zero in the bellmouth, it is concluded that the 500-hertz frequency band is not generated by anything forward of the test section.

At transducer K5, which was located on the cylindrical part of the cone-cylinder model, the fluctuating pressures did not show the sharp peak effect at high subsonic Mach numbers (fig. 15). The maximum values of 27 percent of dynamic pressure for peak-to-peak pressures and 4.4 percent of dynamic pressure for rms pressures are approximately two-thirds of those measured at the test section wall (K4) at Mach 0.75 to 0.8 for the 3.1-percent-porosity test section. At subsonic speeds, the disturbances

at the model were very insensitive to the variations in test section porosity, whereas those on the wall were significantly higher at Mach 0.75 to 0.8 for a porosity of 3.1 percent. At supersonic speeds, the disturbances at the model were similar for the 3.1- and 6.2-percent-porosity test sections, and they were considerably larger than those on the wall. For 0-percent porosity, the disturbances on the model were approximately the same as those on the wall.

Fluctuating pressure data reported in reference 1 for a 3.1-percent-porosity test section are included in figure 15(a). These data were obtained from a transducer (the reference trandsucer) located near the base of a cone-cylinder model, but the model was significantly different from that of the present study and the model blockage was 1.64 percent. The data of reference 1 showed the same trends with Mach number, but the amplitudes were much less than those for transducer K5 with the porous test sections. However, there was good agreement for the nonporous test section at supersonic speeds. These results suggest that the pressure amplitudes measured on the model in a porous test section may be dependent on model configuration variables such as model blockage.

The spectral displays for transducer K5 are shown in figure 16. At Mach 0.70 and 0.80 (figs. 16(a) and (b), respectively) results were similar to those presented for the K4 transducer (figs. 8(a) and (b)) except at high frequencies. At Mach 0.90 (fig. 16(c)), high-frequency disturbances at K5 were much more prominent than on the wall (fig. 8(c)). At supersonic speeds, the high frequencies were also more prominent (compare fig. 16(d) with 8(d)). At 0-percent porosity, the 500 hertz disturbance was not as prominent on the model, but again there were larger high-frequency disturbances (compare fig. 16(e) with 8(e)). Also, at 6.2-percent (fig. 16(f)), there were greater high-frequency disturbances than on the wall (fig. 8(f)). These high-frequency disturbances constitute a significant disturbance on the centerline of the tunnel and are the major factor in the considerably larger fluctuating pressures that were obtained for transducer K5 at supersonic Mach numbers.

A test was made of a modified 8-foot (2.438-m) test section that had perforations on the floor and ceiling plates upstream of the 8-foot (2.438-m) section (fig. 4). Schlieren photographs presented in figure 17 show how the test section flow is influenced by these perforations upstream of the schlieren windows. At Mach 0.988 (fig. 17(a)), the crosshatched appearance results from the intersections of the high-intensity sound waves emitting from the perforations. Similar wave patterns are illustrated in reference 7 for air flowing over a transverse slot. Figure 17(b), which is for a Mach number of 1.388, shows these disturbances being propagated at the Mach angle. Obviously, these disturbances would have no effect on a wind tunnel model at this Mach number if the model were small enough to be located upstream of the Mach line propagating from the beginning of the perforations. Resonant frequencies similar to those in

the 2000- to 8000-hertz band shown in figure 16 can be predicted from the data in reference 7. For this prediction, a 1.57-inch (3.98-cm) slot length (the length of a rectangle of the same area and width as the perforation in the tunnel) would be used.

Transducer K6, located in the diffuser of the tunnel, recorded the highest pressure disturbances of any of the transducers (fig. 18). At Mach 2.0, it indicated a peak-to-peak pressure of 88 percent of dynamic pressure and an rms pressure of 11.5 percent of dynamic pressure. The level of pressure fluctuations decreased as the Mach number decreased until it reached a minimum value at Mach 1.0. This indicates that the fluctuating pressures in the diffuser for the supersonic Mach numbers are related to the terminal shock strength. Below Mach 1.0, the second throat is constricted to control the test section Mach number, and the increase in the fluctuating pressures presumably is due to flow separation from the rear surfaces of the second throat doors rather than to any disturbance in the test section. Reference 2 indicates that the fluctuating flows in the test section may be triggered by unsteady flow in the subsonic diffuser. However, since the second throat is choked for the 8- by 6-foot supersonic wind tunnel at the subsonic Mach numbers presented, it seems that the diffuser is not the source in this case. The only effect of test section porosity was evident near Mach 0.8, where a somewhat greater amplitude existed with 0-percent porosity. In figure 19, the spectral displays for transducer K6 show disturbances at several discrete frequencies (including 500 and 800 Hz) at all subsonic Mach numbers; however, at supersonic speeds (fig. 19(d)), the 800-hertz peak is shown to be the predominant one.

An additional test was made without the cone-cylinder model installed in the test section to determine if the model had contributed to the pressure disturbances at the test section walls. A test section porosity of 3.1 percent was used for this test. Data presented in figure 20 for transducers K2, K3, and K4 compare the pressure disturbances with and without the cone-cylinder model installed. The results show that the model had little effect on the pressure disturbances on the tunnel wall. Spectral displays for the empty 3.1-percent-porosity test section are shown in figure 21. The data for transducers K2 and K3 are for Mach 0.775, and that for transducer K4 is for Mach 0.775 and 1.10. At Mach 0.775 (figs. 21(a) to (c)), results were similar to those shown in previous figures. At Mach 1.10 (fig. 21(d)), the prominent frequencies were 800, 2000, and 4000 hertz. In order to show the power available in the various frequency bands, the power spectral density displays for these conditions are presented in figure 22. The power spectral density displays show a high-energy level in the 500-hertz band at Mach 0.775. Transducer K4 shows a large increase in the 800-hertz signal at Mach 1.10 and additional power peaks in the higher frequency range of 1500 to 2000 hertz, the limit of the power spectral analysis. It is expected that additional power peaks at frequencies above 2000 hertz are also present because of the perturbations shown in the spectral displays of figure 21.

An additional phenomenon indicated by the results is shown in figure 23, in which the peak-to-peak fluctuating pressure amplitudes for transducers K1 to K5 are plotted against the rms fluctuating pressure for each test section porosity. For white noise, the ratio of Δp_{p-p} to Δp_{rms} is approximately 6, and a pure sine wave has a ratio of 2.8. Ratios of 7.3, 7.1, and 6.3 were obtained for porosities of 6.2, 3.1, and 0 percent (figs. 23(a) to (c)), respectively. Apparently, the ratios are above the average white-noise ratios because of the unusual wave shape and frequency distribution of the fluctuating pressures that occur in the test section.

When the fluctuating pressures measured in the 8- by 6-foot supersonic wind tunnel are compared with those measured in the tunnels of references 2 to 5, the following observations are noted:

(1) All the test sections have a local porosity of approximately 6 percent, and all have fluctuating pressure with amplitude peaks at Mach numbers from 0.6 to 0.85.

(2) The perforations in each of the test sections are inclined 60° forward.

(3) References 3 to 5 also reported rms pressure peaks at a frequency of about 500 hertz.

(4) Data were presented only for frequencies up to 1200 hertz except for the 8- by 6-foot supersonic wind tunnel and reference 5, where the maximum frequencies were 10 000 and 6000 hertz, respectively.

(5) All walls of the test sections were perforated except for the tunnel reported in reference 4, which had solid side walls.

Reference 4 presents test results on three test section configurations for which the predominant disturbance at 500 hertz that existed on the test section walls in the high subsonic Mach number range was eliminated when the porosity was decreased. The decreased porosity configurations were a test section with 0-percent porosity, a test section with 0-percent porosity on only one wall, and a test section with the porosity of top and bottom walls reduced by covering the upstream one-third of each hole by external sliding plates. Similarly, in the 8- by 6-foot supersonic wind tunnel, decreasing the test section porosity to 0 percent reduced the fluctuating pressures in the 500-hertz frequency band to 40 percent of the peak values. However, increasing the average test section porosity from 3.1 to 6.2 percent reduced the magnitude of this disturbance a similar amount.

It is concluded from the foregoing that several complementary phenomena are occurring in the test section simultaneously that cause the pressure resonance. One of these phenomena may be a transverse resonance between opposite walls of the test section which could be initiated by the flow through the perforations. The frequency of a transverse resonance can be expressed by

$$f = n\frac{a}{x}\left(1 - M^2\right)^{1/2}$$

where f is the frequency in hertz, n equals 1, 2, 3, . . ., a is the speed of sound at ambient test section conditions, x is the dimension of the test section, and M is the Mach number. For the 6-foot (1.829-m) width of the 8- by 6-foot supersonic wind tunnel, the fourth harmonic (n = 4) would provide a resonance at approximately 500 hertz. For other tunnels, the various different Mach numbers and frequencies at which the resonant peaks occur might be associated with the different test section dimensions.

SUMMARY OF RESULTS

Pressure perturbations were observed to exist in the test section of the 8- by 6-foot supersonic wind tunnel. Therefore, dynamic pressure measurements were made with flush-mounted transducers located in the bellmouth, in the test section, in the tunnel diffuser, and on a 0.284-percent-blockage cone-cylinder model mounted in the test section. This investigation yielded the following results:

1. The maximum amplitude of the pressure perturbations in the test section occurred at Mach numbers near 0.75. At this speed, the principal disturbance occurred at a frequency of about 500 hertz, and a secondary disturbance existed at 800 hertz. At supersonic speeds, there were less prominent disturbances at several frequencies from 800 to 8000 hertz. The disturbance at 800 hertz originated from the compressor, and the 500-hertz disturbance appeared to be a flow resonance within the porous region of the test section. The high-frequency perturbations in the range of 2000 to 8000 hertz appeared to be generated by the holes in the test section wall and constituted a significant disturbance on the test section centerline at supersonic Mach numbers. The pressure oscillations in the subsonic diffuser did not appear to influence the test section perturbations.

2. The maximum perturbation on the test section wall was observed near Mach 0.75 for a test section average porosity of 3.1 percent. Root-mean-square pressures reached a maximum of 6.3 percent of tunnel dynamic pressure. These high-pressure perturbations are similar to those that were reported for other transonic wind tunnels of a similar wall geometry. Varying the test section average porosity to 6.2 or to 0 percent reduced this disturbance to approximately 40 percent of its maximum value.

3. The pressure perturbations on a low-blockage model were not significantly affected by changes in test section porosity from 3.1 to 6.2 percent. At supersonic speeds, these perturbations were significantly greater than those obtained with the same low-blockage model in a nonporous test section. At all speeds, these perturbations

were greater than those reported previously for a high-blockage model in a 3.1-percent-porosity test section.

Lewis Research Center,
National Aeronautics and Space Administration,
Cleveland, Ohio, February 9, 1970,
720-03.

REFERENCES

1. Blaha, Bernard J.: Wind Tunnel Investigation of Fluctuating Pressures on a 1/10-Scale Centaur Model at Transonic Speeds. NASA TM X-1574, 1968.
2. Robertson, J. E.: Measurement of the Pressure Fluctuations in the Test Section of the 1-Foot Transonic Tunnel in the Frequency Range from 5 to 1250 cps. ARO, Inc. (AEDC-TDR-62-109) May 1962.
3. Chevalier, H. L.; and Todd, H. E.: Measurement of the Pressure Fluctuations in the Test Section of the 16-Foot Transonic Circuit in the Frequency Range from 5 to 1000 cps. ARO, Inc. (AEDC-TN-61-51) May 1961.
4. Christophe, J. M.; and Loniewski, J. M.: Reduction of Pressure Fluctuations in a Transonic Test-Section. TP no. 567, ONERA, 1968.
5. Riddle, C. D.: Investigation of Free-Stream Fluctuating Pressures in the 16-Foot Tunnels of the Propulsion Wind Tunnel Facility. ARO, Inc. (AEDC-TR-67-167, DDC No. AD-818388), Aug. 1967.
6. Mitchell, Glenn A.: Blockage Effects of Cone-Cylinder Bodies on Perforated Wind Tunnel Wall Interference. NASA TM X-1655, 1968.
7. Krishnamurty, K.: Acoustic Radiation from Two-Dimensional Rectangular Cutouts in Aerodynamic Surfaces. NACA TN 3487, 1955.

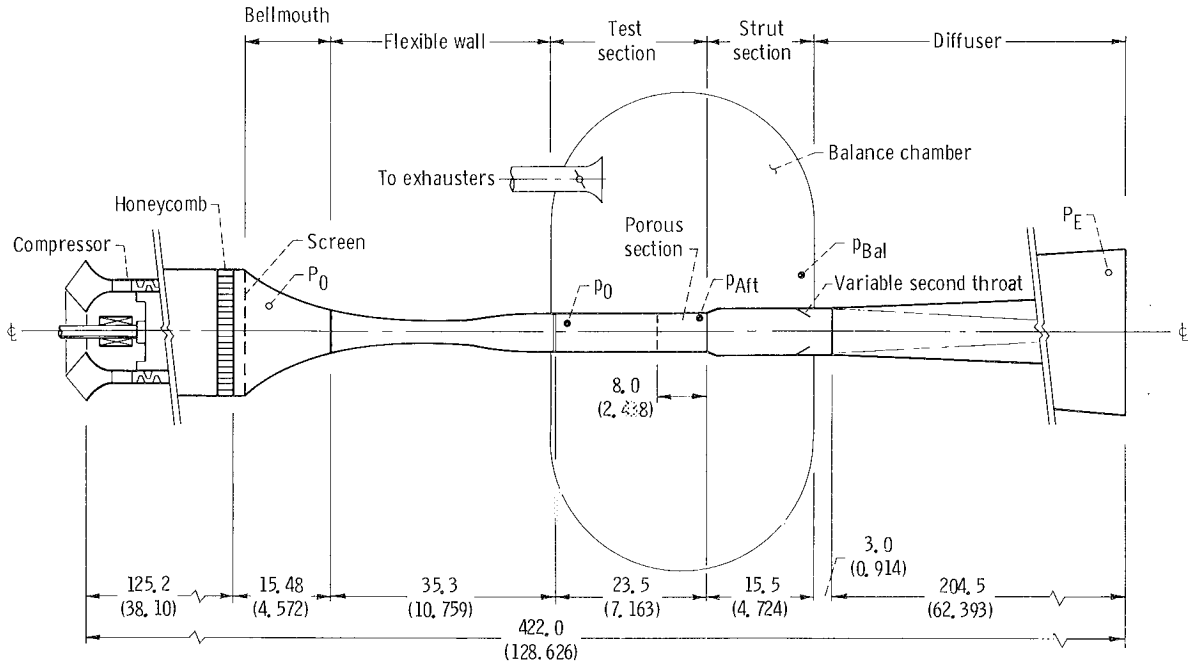

Figure 1. - Plan view of 8- by 6-foot supersonic wind tunnel. All dimensions are in feet (m).

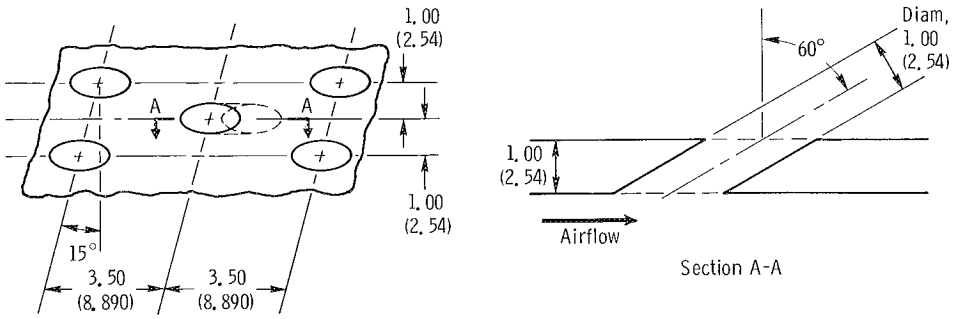

Figure 2. - Perforation detail for 8-by 6-foot supersonic wind tunnel. All dimensions are in inches (cm).

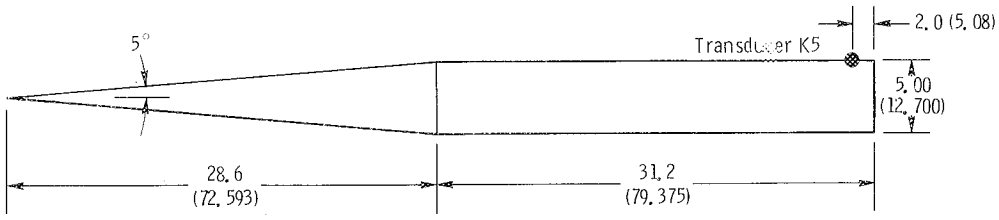

Figure 3. - Dimensions of 5° half-angle cone-cylinder model. All dimensions are in inches (cm).

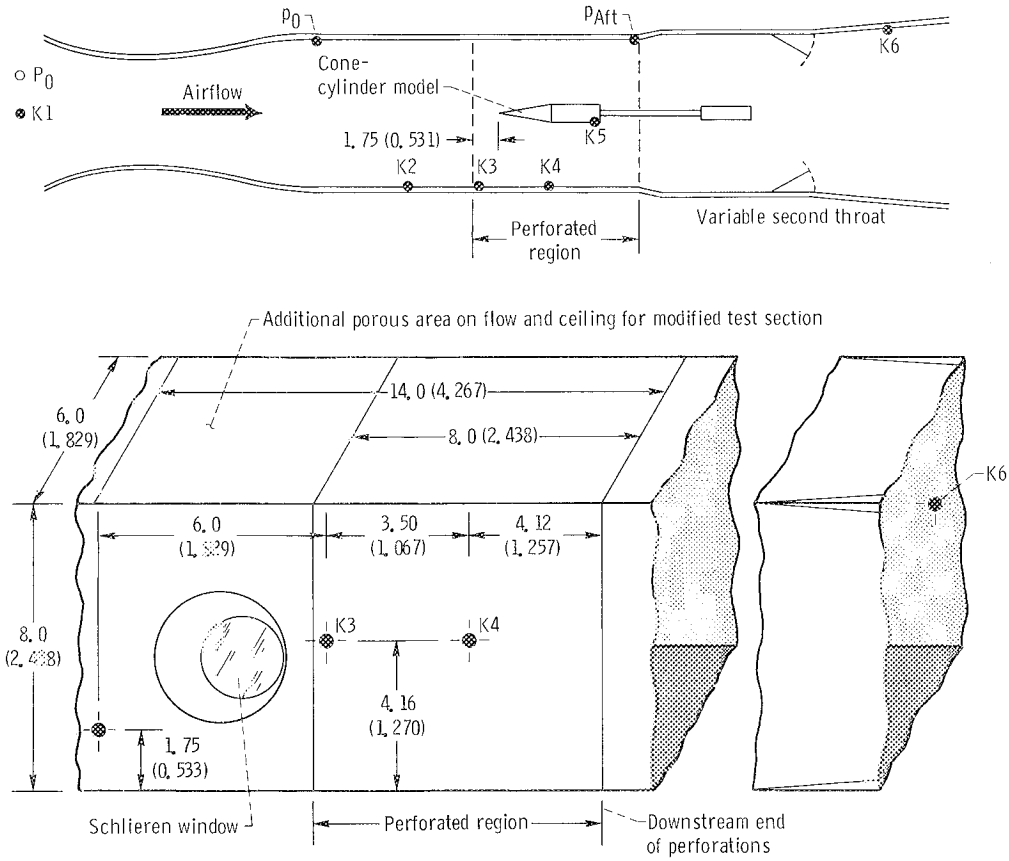

Figure 4. - Location of dynamic pressure transducers in 8- by-6 foot supersonic wind tunnel. All dimensions are in feet (m).

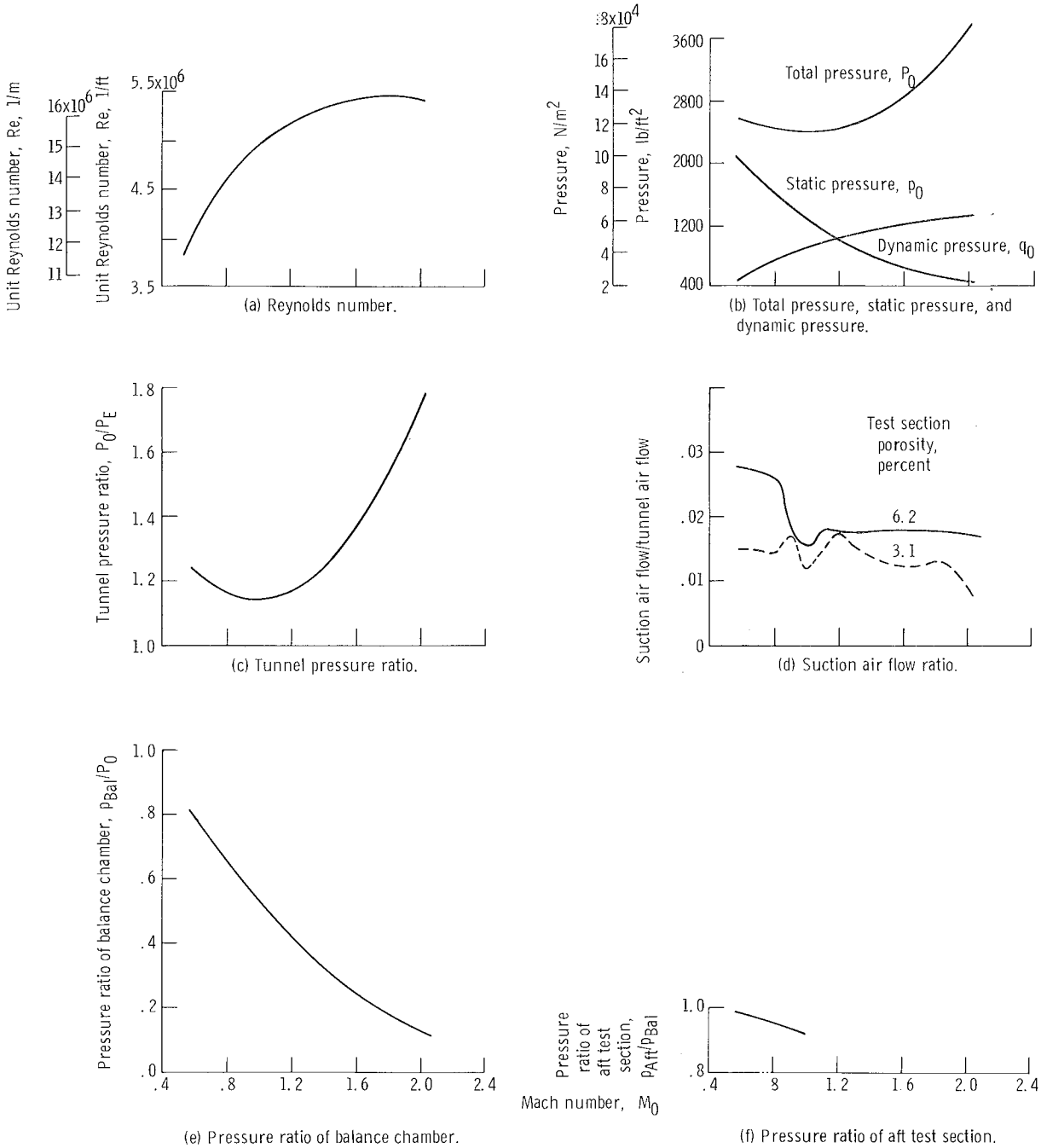

Figure 5. - Flow parameters of 8- by 6-foot supersonic wind tunnel for Mach numbers from 0.56 to 2.07.

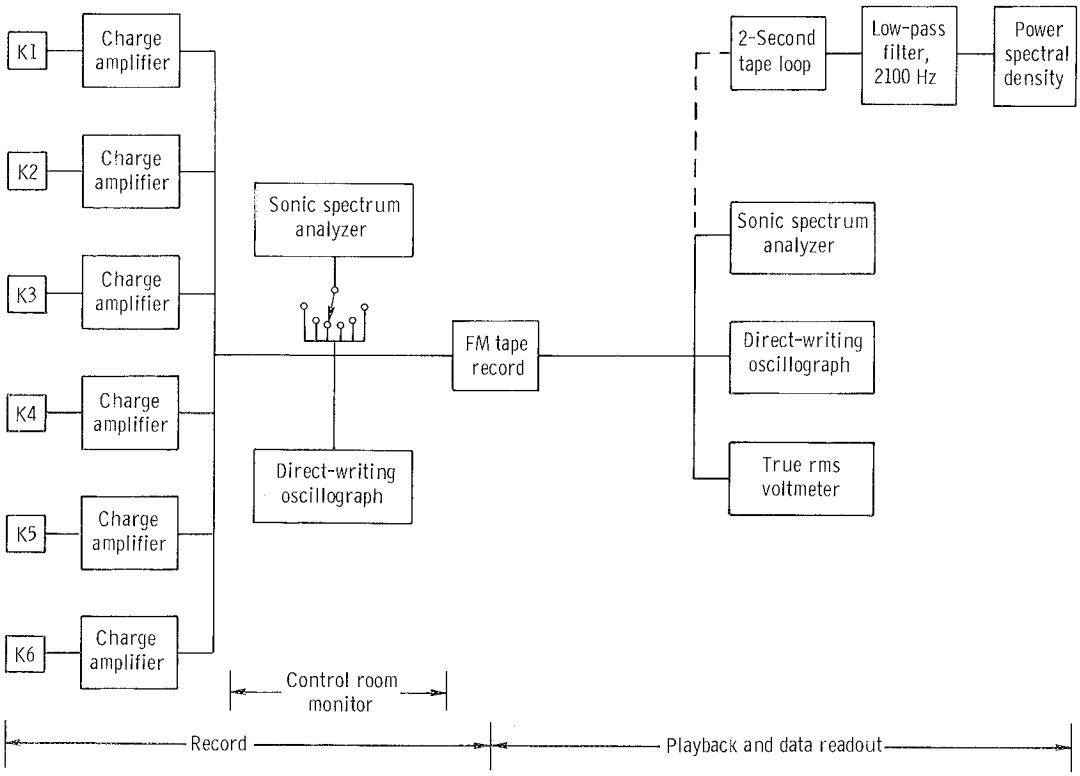

Figure 6. - Equipment for recording and data playback.

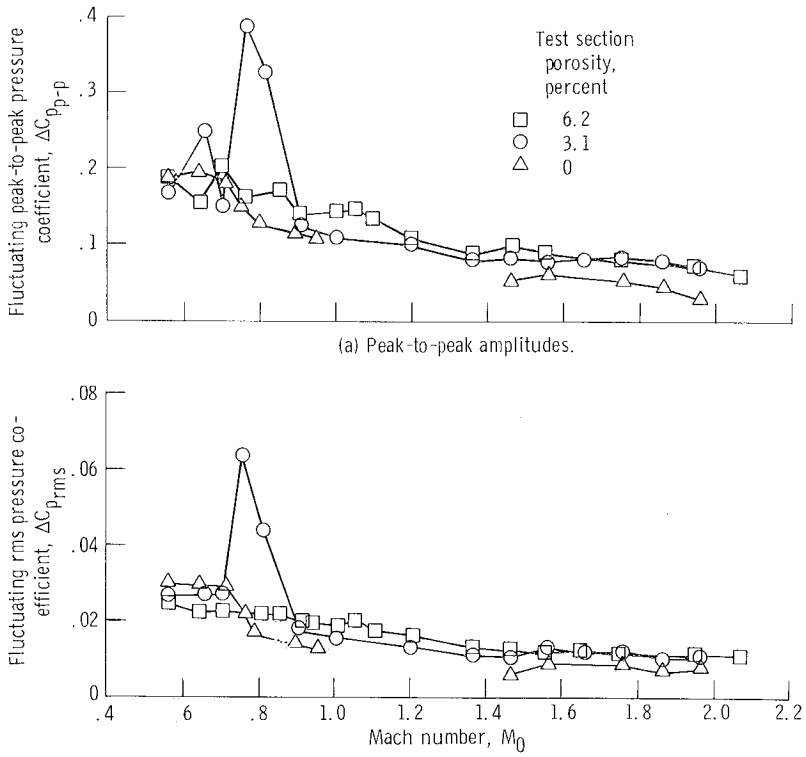

Figure 7. - Effect of Mach number on fluctuating pressure coefficient for transducer K4 located in porous region of test section.

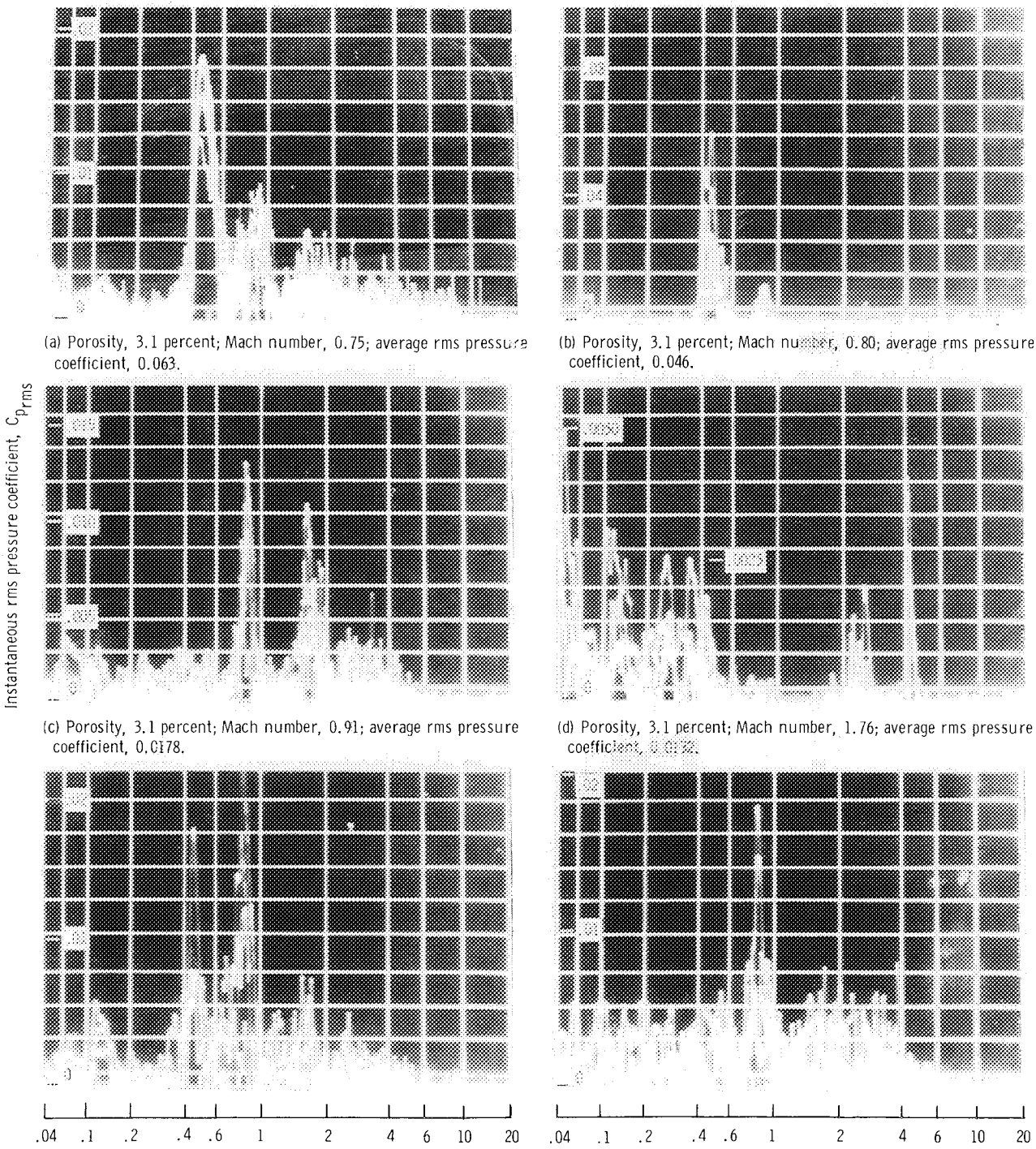

(a) Porosity, 3.1 percent; Mach number, 0.75; average rms pressure coefficient, 0.063.

(b) Porosity, 3.1 percent; Mach number, 0.80; average rms pressure coefficient, 0.046.

(c) Porosity, 3.1 percent; Mach number, 0.91; average rms pressure coefficient, 0.0178.

(d) Porosity, 3.1 percent; Mach number, 1.76; average rms pressure coefficient, 0.0132.

(e) Porosity, 0 percent; Mach number, 0.75; average rms pressure coefficient, 0.025.

(f) Porosity, 6.2 percent; Mach number, 0.80; average rms pressure coefficient, 0.023.

Figure 8. - Spectral displays of fluctuating pressures for transducer K4.

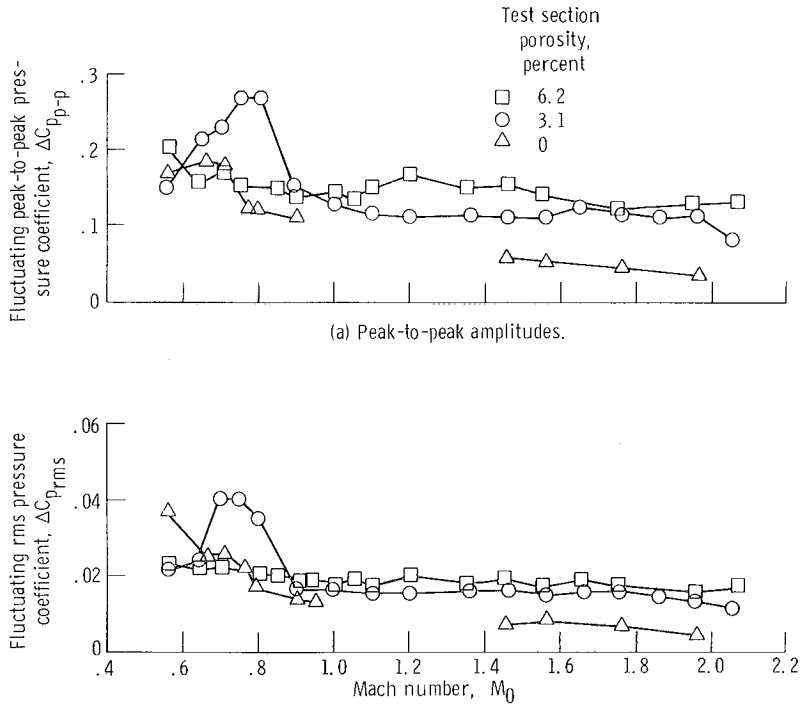

(a) Peak-to-peak amplitudes.

(b) Root-mean-square amplitudes.

Figure 9. - Effect of Mach number on fluctuating pressure coefficients for transducer K3 located at beginning of porous test section.

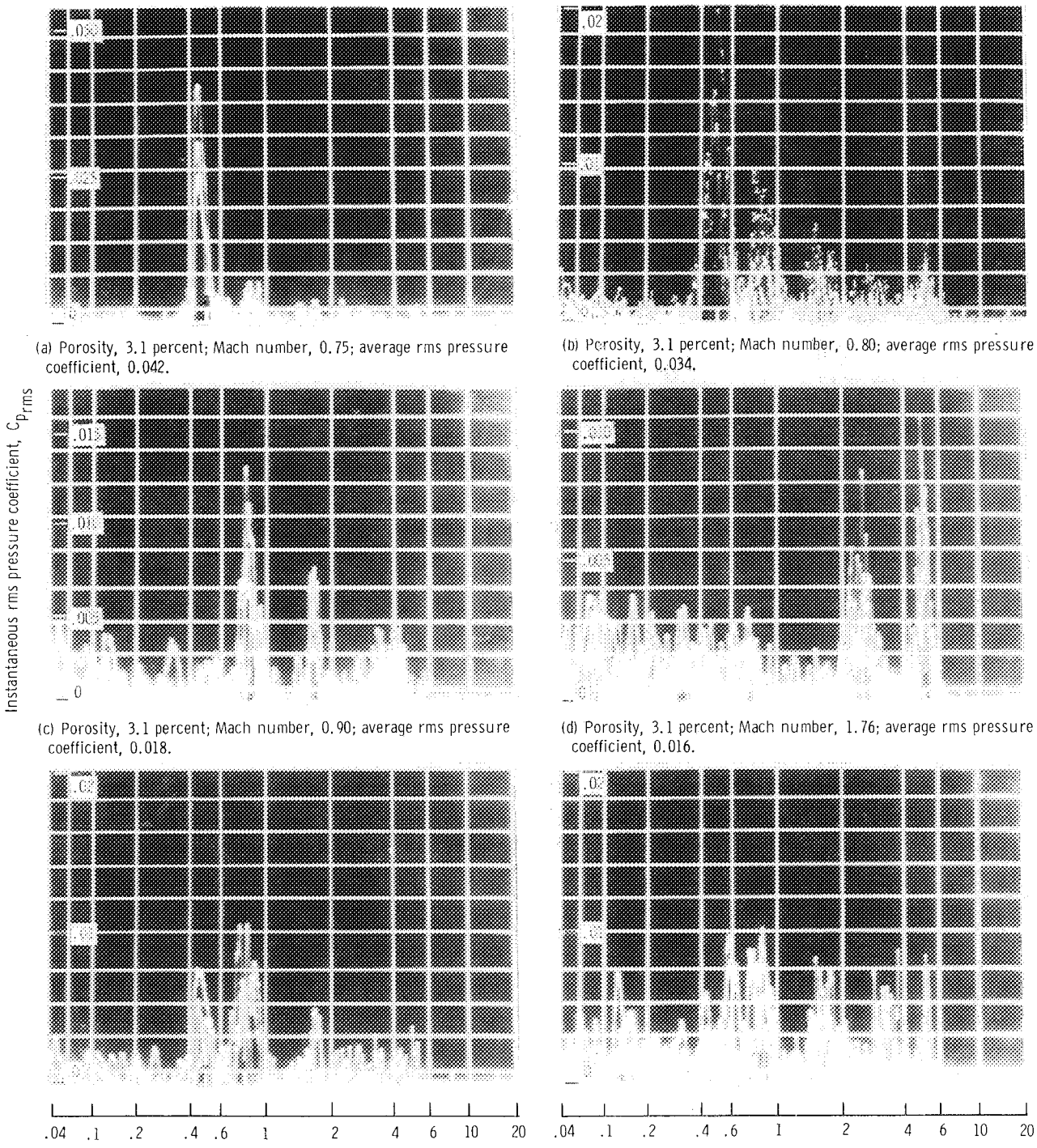

(a) Porosity, 3.1 percent; Mach number, 0.75; average rms pressure coefficient, 0.042.

(b) Porosity, 3.1 percent; Mach number, 0.80; average rms pressure coefficient, 0.034.

(c) Porosity, 3.1 percent; Mach number, 0.90; average rms pressure coefficient, 0.018.

(d) Porosity, 3.1 percent; Mach number, 1.76; average rms pressure coefficient, 0.016.

(e) Porosity, 0 percent; Mach number, 0.79; average rms pressure coefficient, 0.0175.

(f) Porosity, 6.2 percent; Mach number, 0.80; average rms pressure coefficient, 0.022.

Figure 10. - Spectral displays of fluctuating pressures for transducer K3.

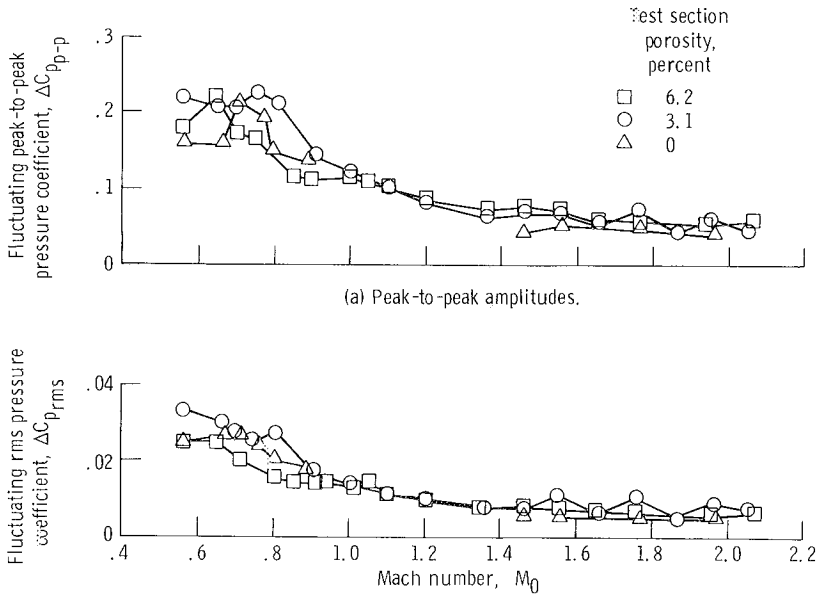

Figure 11. - Effect of Mach number on fluctuating pressure coefficients for transducer K2 located in solid portion of test section.

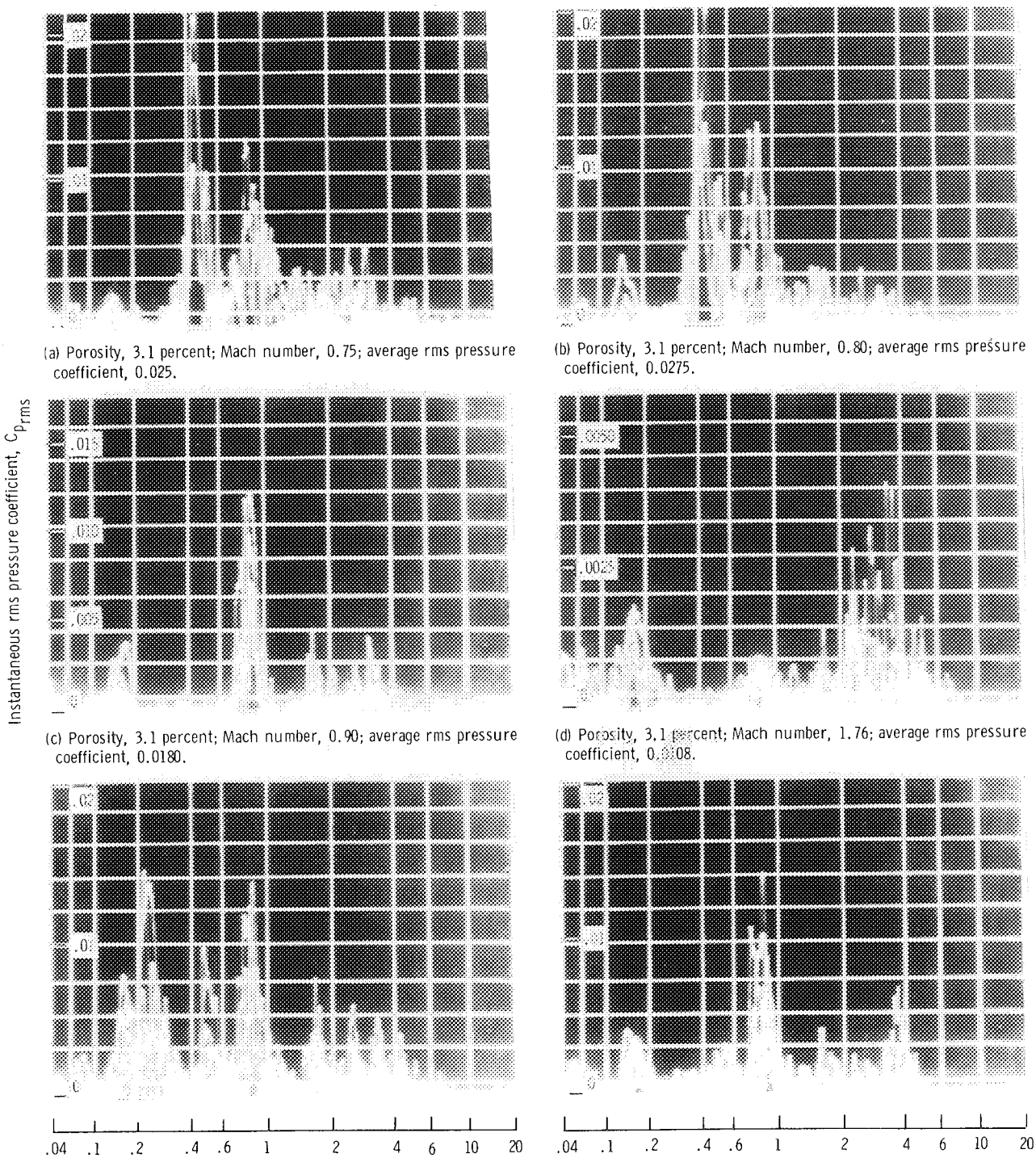

(a) Porosity, 3.1 percent; Mach number, 0.75; average rms pressure coefficient, 0.025.

(b) Porosity, 3.1 percent; Mach number, 0.80; average rms pressure coefficient, 0.0275.

(c) Porosity, 3.1 percent; Mach number, 0.90; average rms pressure coefficient, 0.0180.

(d) Porosity, 3.1 percent; Mach number, 1.76; average rms pressure coefficient, 0.0108.

(e) Porosity, 0 percent; Mach number, 0.79; average rms pressure coefficient, 0.022.

(f) Porosity, 6.2 percent; Mach number, 0.80; average rms pressure coefficient, 0.0172.

Figure 12. - Spectral displays of fluctuating pressures for transducer K2.

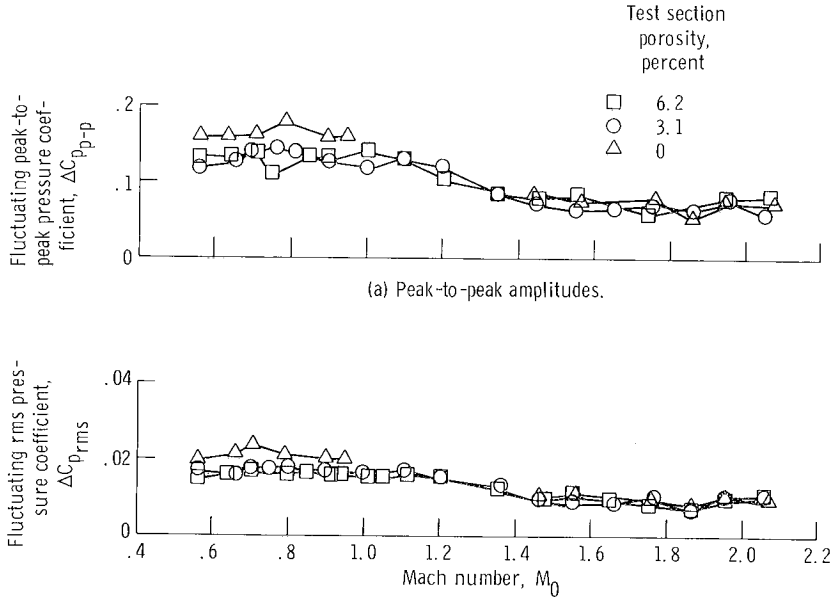

Figure 13. - Effect of Mach number on fluctuating pressure coefficients for bell-mouth transducer K1.

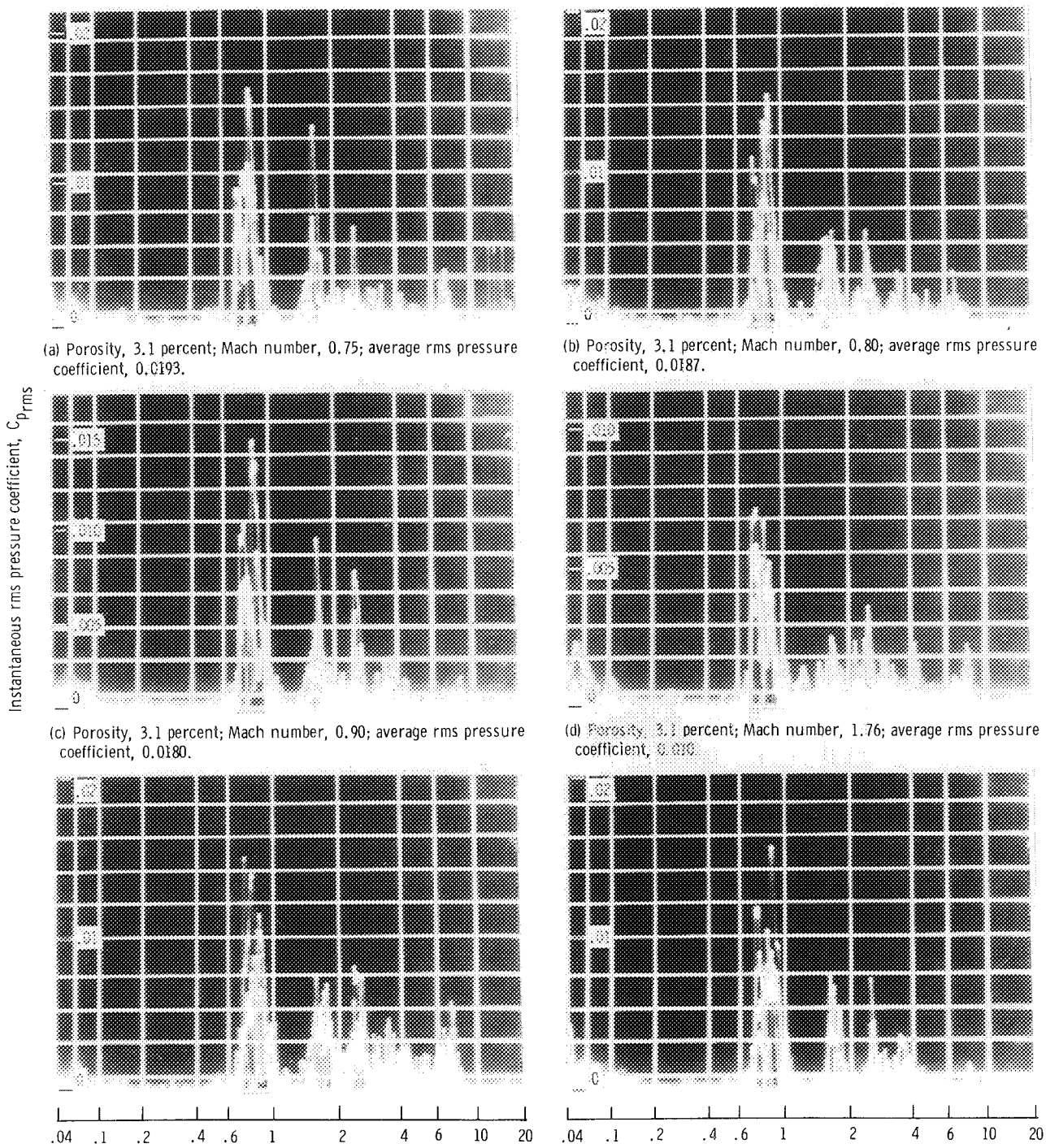

(a) Porosity, 3.1 percent; Mach number, 0.75; average rms pressure coefficient, 0.0193.

(b) Porosity, 3.1 percent; Mach number, 0.80; average rms pressure coefficient, 0.0187.

(c) Porosity, 3.1 percent; Mach number, 0.90; average rms pressure coefficient, 0.0180.

(d) Porosity, 3.1 percent; Mach number, 1.76; average rms pressure coefficient, 0.0170.

(e) Porosity, 0 percent; Mach number, 0.80; average rms pressure coefficient, 0.0216.

(f) Porosity, 6.2 percent; Mach number, 0.80; average rms pressure coefficient, 0.0172.

Figure 14. - Spectral displays of fluctuating pressures for transducer K1.

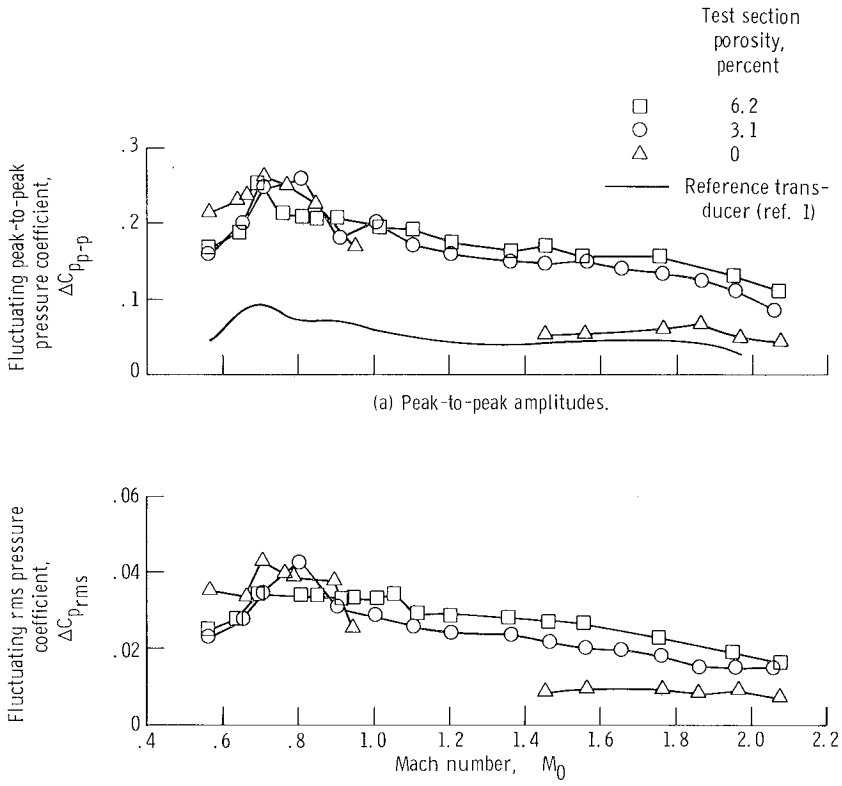

Figure 15. - Effect of Mach number on fluctuating pressure coefficients for model transducer K5.

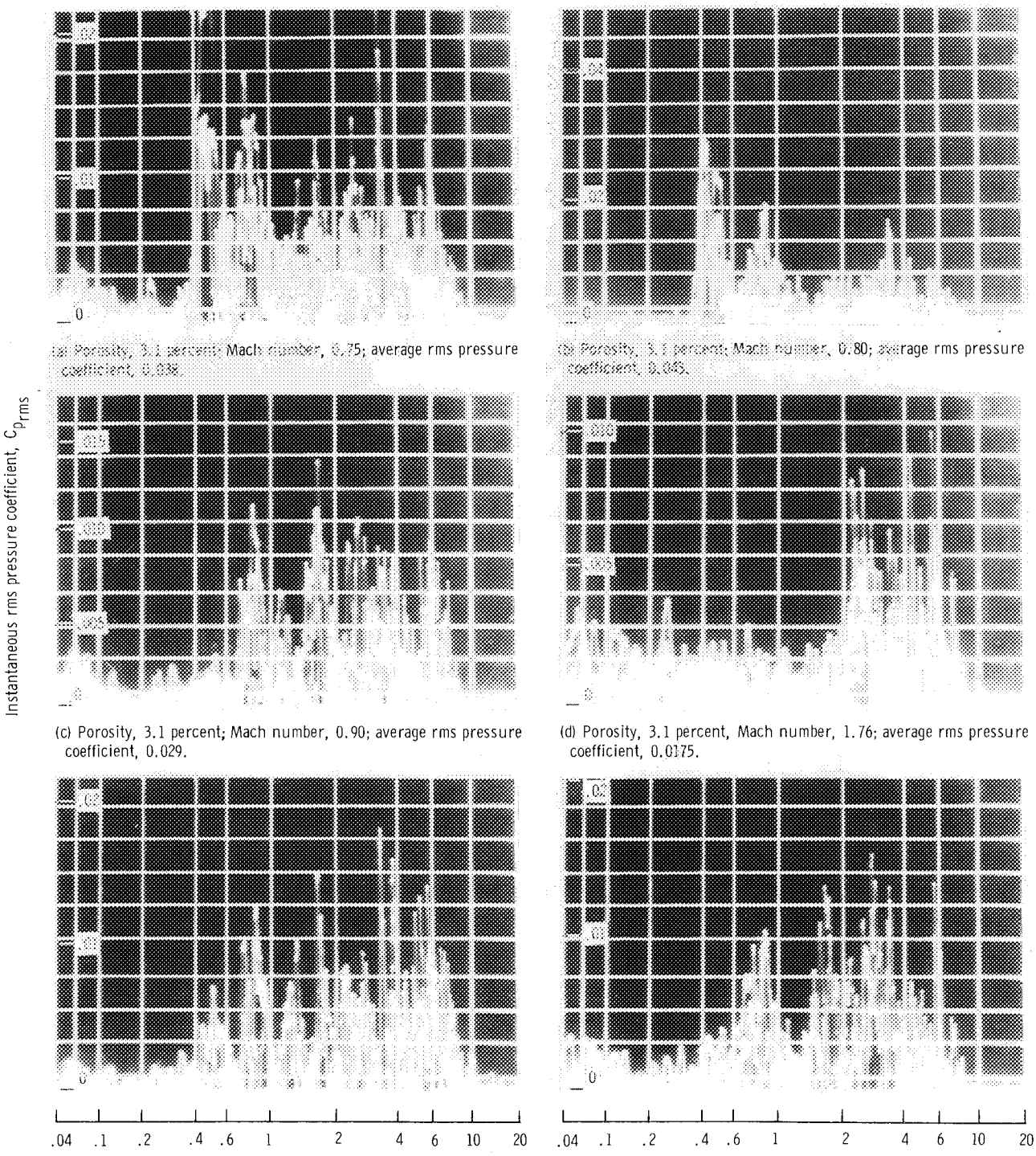

(a) Porosity, 3.1 percent; Mach number, 0.75; average rms pressure coefficient, 0.038.

(b) Porosity, 3.1 percent; Mach number, 0.80; average rms pressure coefficient, 0.045.

(c) Porosity, 3.1 percent; Mach number, 0.90; average rms pressure coefficient, 0.029.

(d) Porosity, 3.1 percent, Mach number, 1.76; average rms pressure coefficient, 0.0175.

(e) Porosity, 0 percent; Mach number, 0.75; average rms pressure coefficient, 0.042.

(f) Porosity, 6.2 percent; Mach number, 0.80; average rms pressure coefficient, 0.03.

Figure 16. - Spectral displays of fluctuating pressures for transducer K5.

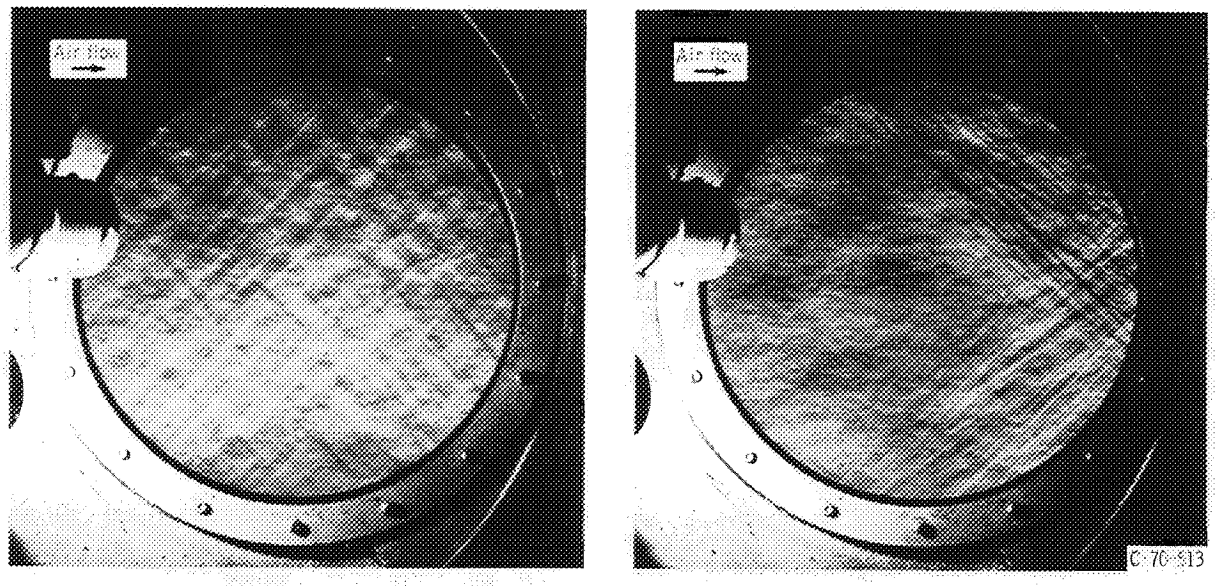

(a) Mach number, 0.998.

(b) Mach number, 1.388.

Figure 17. - Effects of porosity on wind tunnel flow in modified test section as shown by schlieren. Horizontal knife with 1-microsecond-duration spark light source.

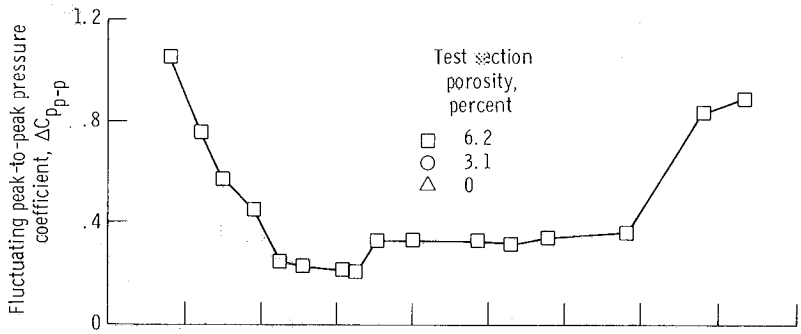

(a) Peak-to-peak amplitudes.

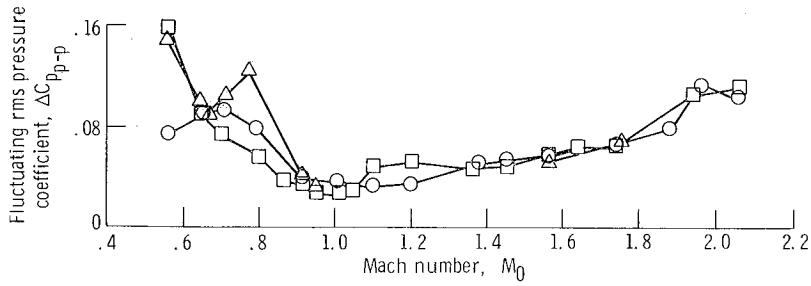

(b) Root-mean-square amplitudes.

Figure 18. - Effect of Mach number on fluctuating pressure coefficients for diffuser transducer K6.

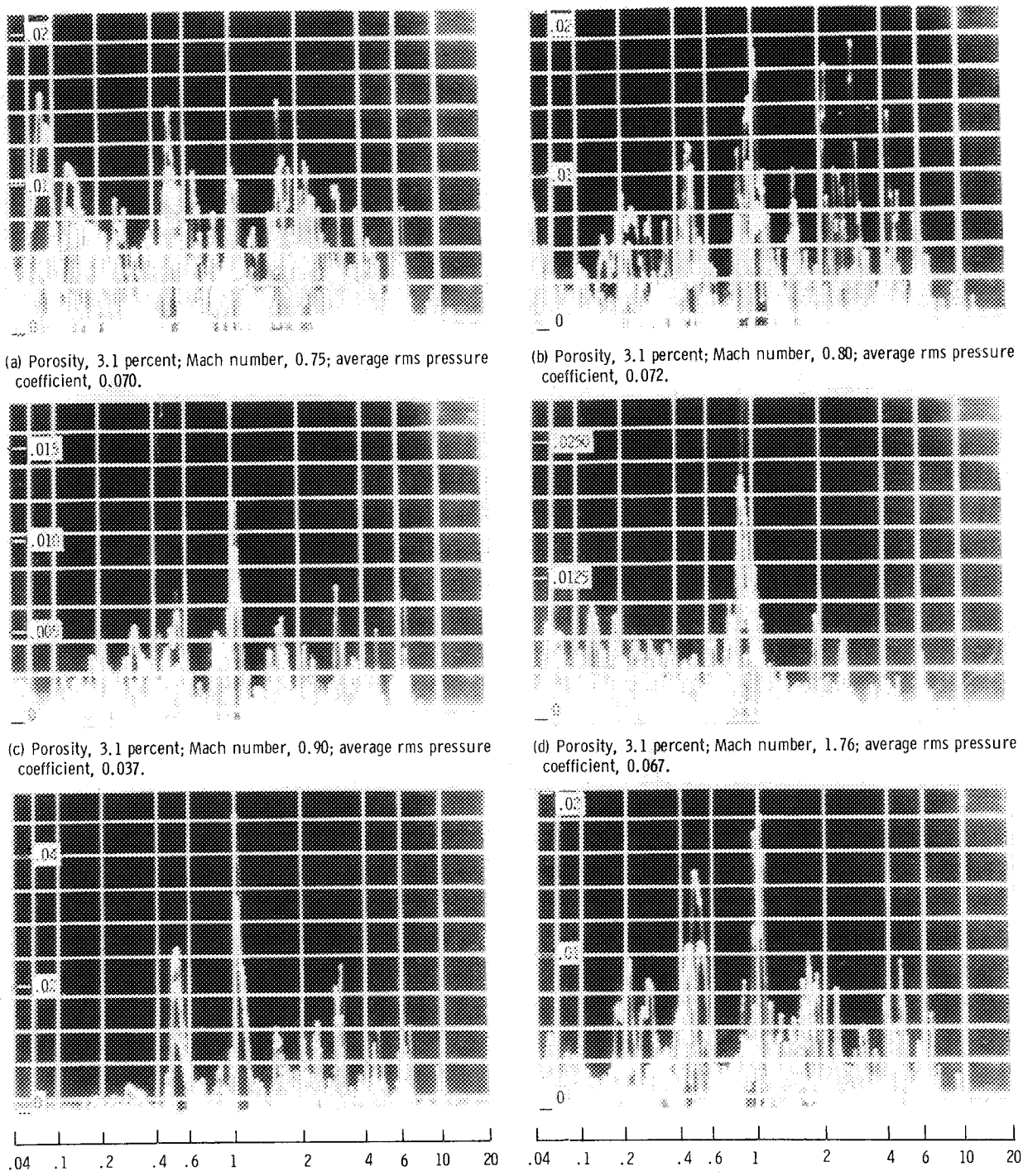

(a) Porosity, 3.1 percent; Mach number, 0.75; average rms pressure coefficient, 0.070.

(b) Porosity, 3.1 percent; Mach number, 0.80; average rms pressure coefficient, 0.072.

(c) Porosity, 3.1 percent; Mach number, 0.90; average rms pressure coefficient, 0.037.

(d) Porosity, 3.1 percent; Mach number, 1.76; average rms pressure coefficient, 0.067.

(e) Porosity, 0 percent; Mach number, 0.80; average rms pressure coefficient, 0.120.

(f) Porosity, 6.2 percent; Mach number, 0.80; average rms pressure coefficient, 0.058.

Figure 19. - Spectral displays of fluctuating pressures for transducer K6.

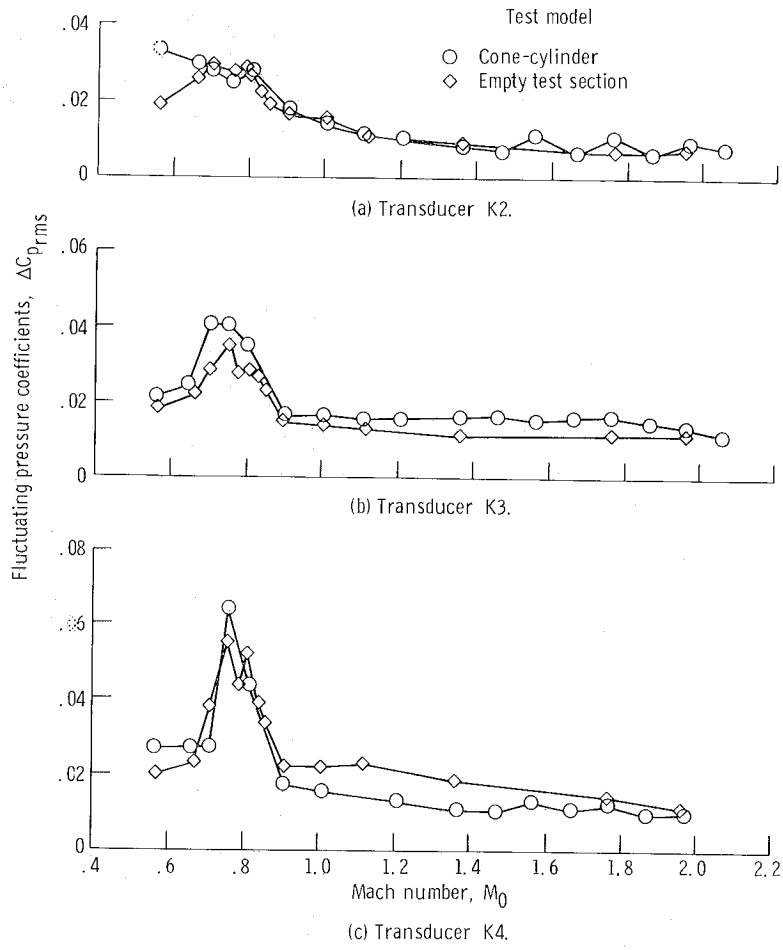

Figure 20. - Effect of model on fluctuating pressure coefficients in 3.1-percent-porosity test section.

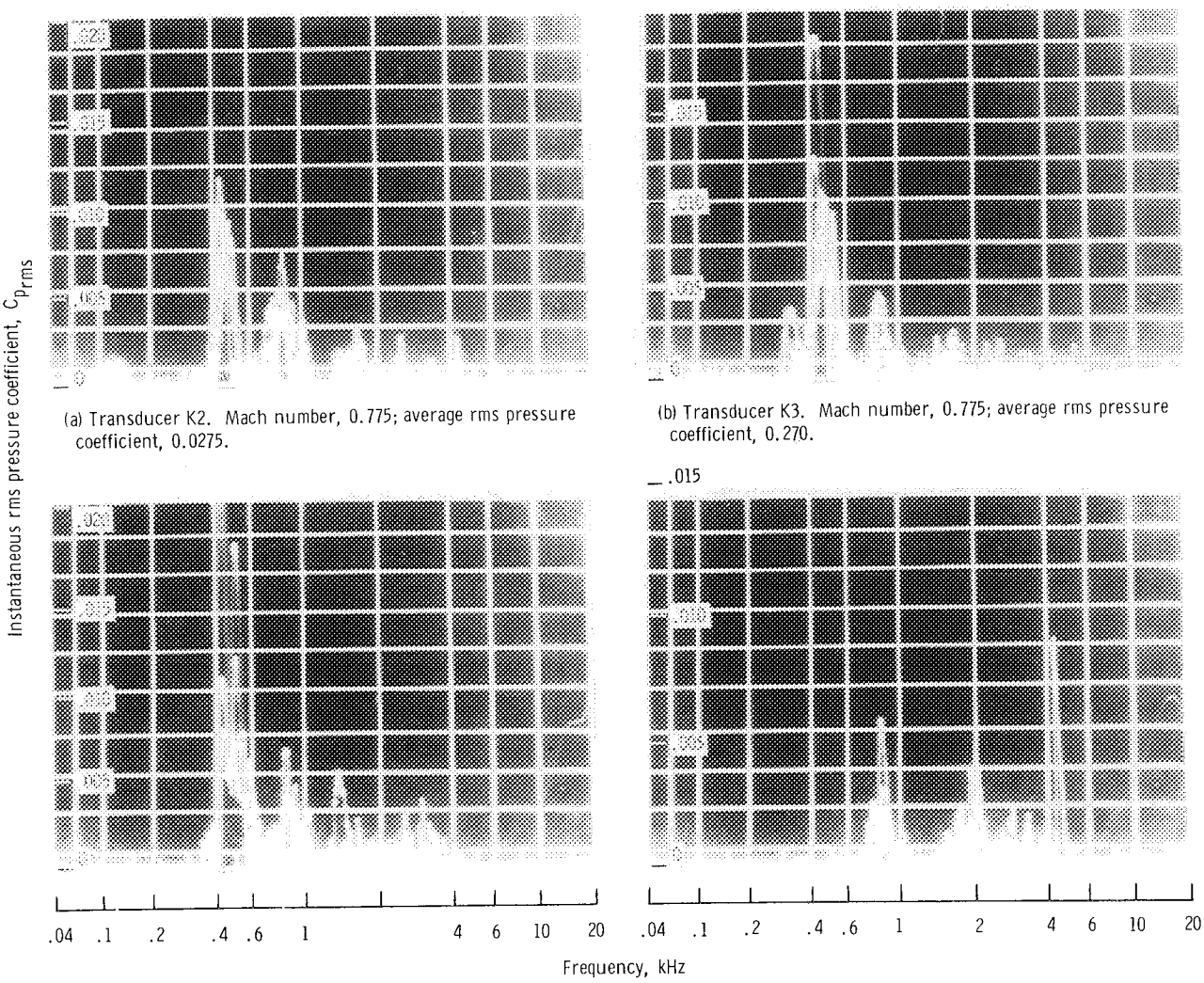

(a) Transducer K2. Mach number, 0.775; average rms pressure coefficient, 0.0275.

(b) Transducer K3. Mach number, 0.775; average rms pressure coefficient, 0.270.

(c) Transducer K4. Mach number, 0.775; average rms pressure coefficient, 0.043.

(d) Tranducer K4. Mach number, 1.10; average rms pressure coefficient, 0.023.

Figure 21. - Spectral displays of fluctuating pressures for empty 3.1-percent-porosity test section.

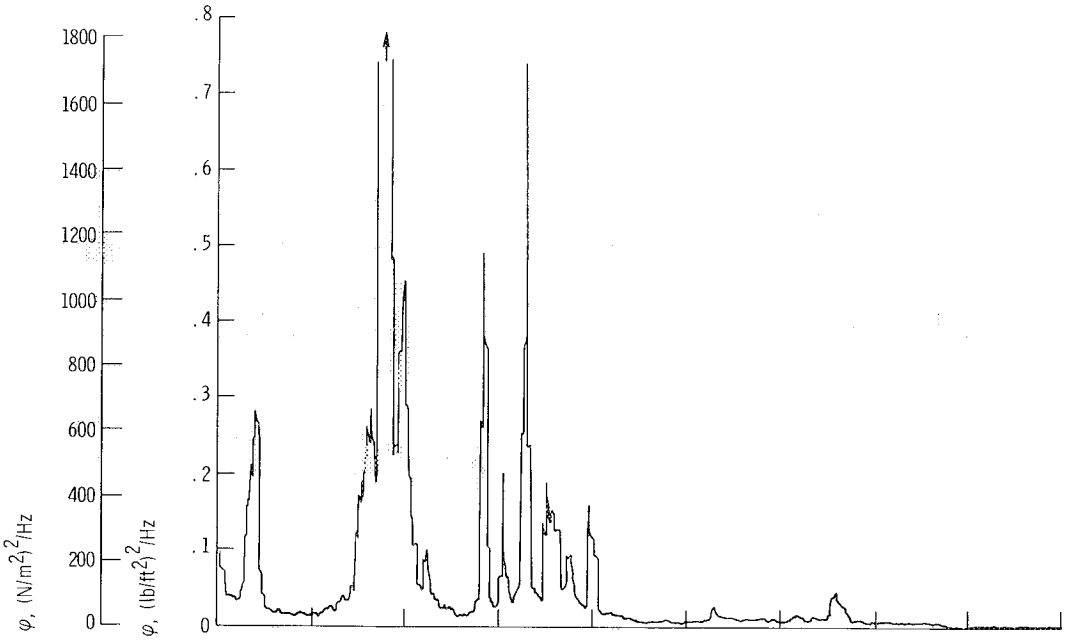

(a) Transducer K2. Mach number, 0.775.

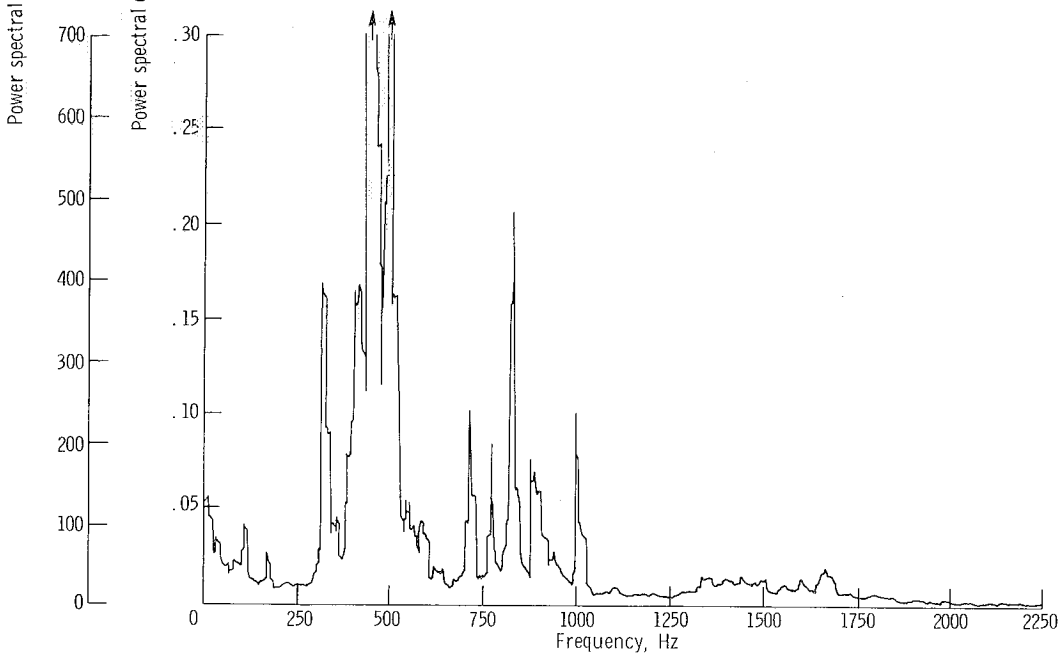

(b) Transducer K3. Mach number, 0.775.

Figure 22. - Power spectral density analysis of fluctuating pressure on test section side wall with 3.1-percent porosity.

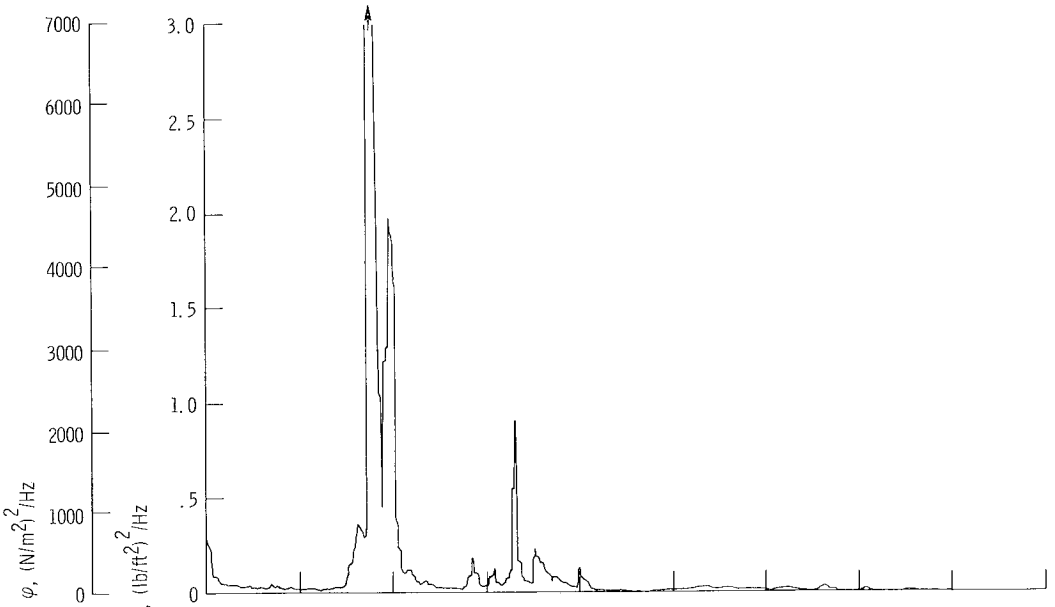

(c) Transducer K4. Mach number, 0.775.

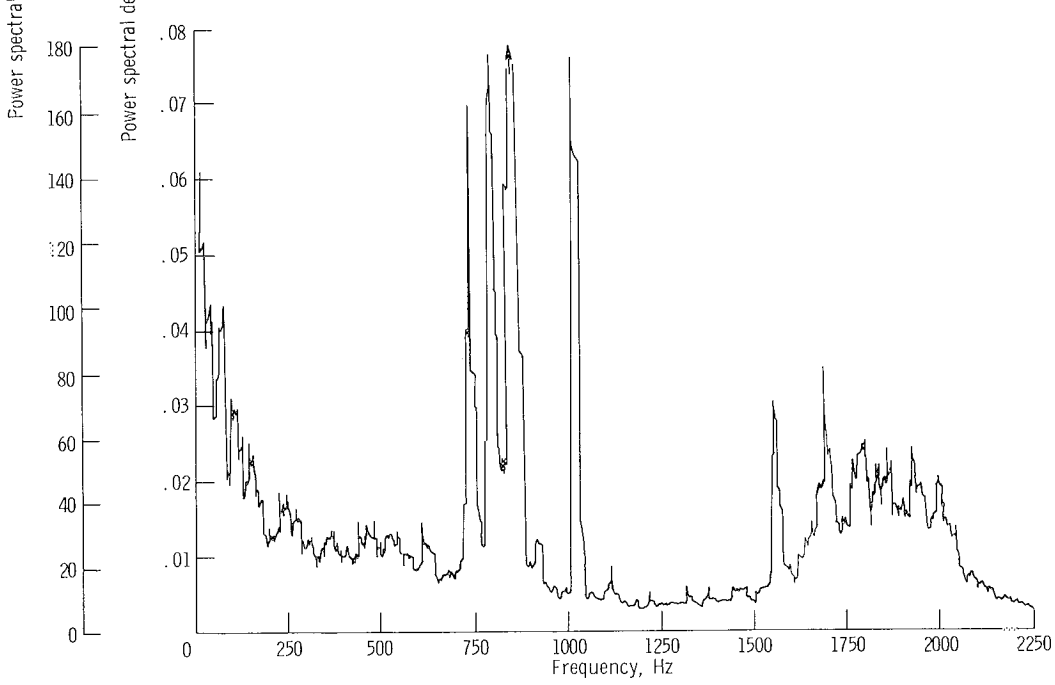

(d) Transducer K4. Mach number, 1.10.

Figure 22. - Concluded.

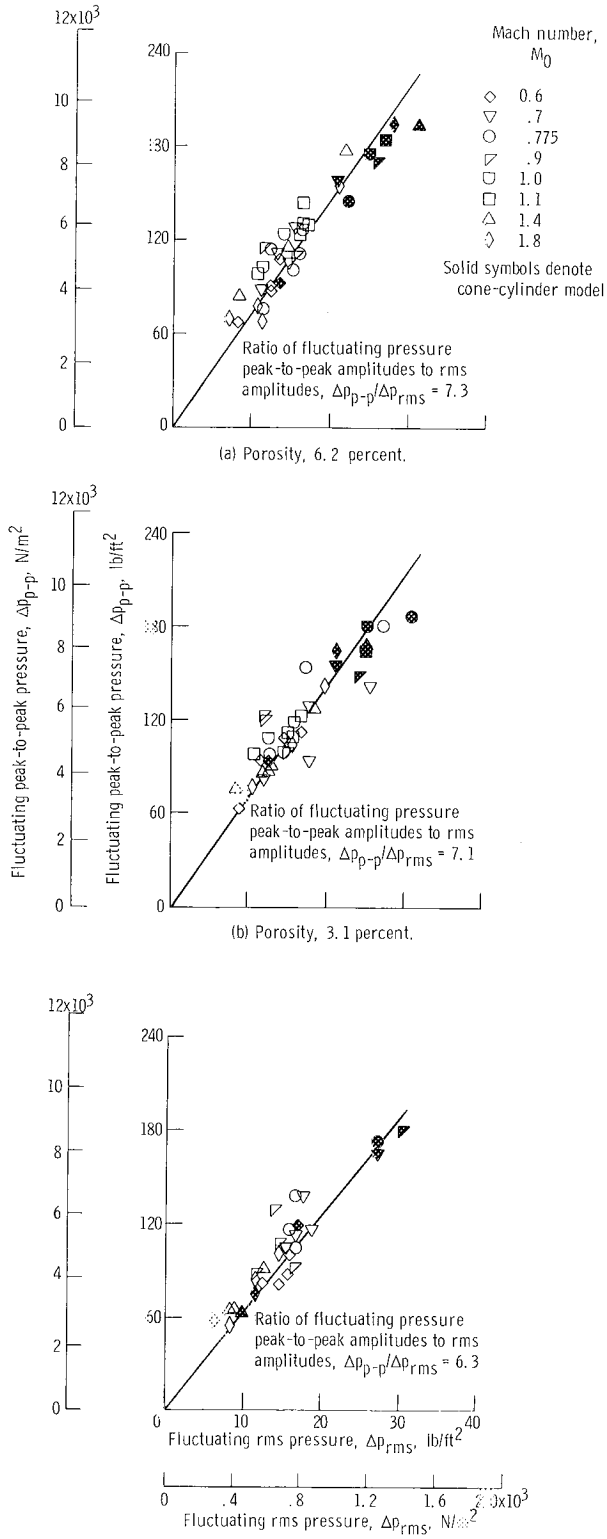

Figure 23. - Effect of test section porosity on ratio of fluctuating pressure peak-to-peak amplitudes to rms amplitudes for transducers K1 to K5.

NASA-Langley, 1970 —— 11 E-5518

NATIONAL AERONAUTICS AND SPACE ADMINISTRATION
WASHINGTON, D.C. 20546
OFFICIAL BUSINESS

FIRST CLASS MAIL

POSTAGE AND FEES PAID
NATIONAL AERONAUTICS AND
SPACE ADMINISTRATION

POSTMASTER: If Undeliverable (Section 158
Postal Manual) Do Not Return

"The aeronautical and space activities of the United States shall be conducted so as to contribute . . . to the expansion of human knowledge of phenomena in the atmosphere and space. The Administration shall provide for the widest practicable and appropriate dissemination of information concerning its activities and the results thereof."

—National Aeronautics and Space Act of 1958

NASA SCIENTIFIC AND TECHNICAL PUBLICATIONS

TECHNICAL REPORTS: Scientific and technical information considered important, complete, and a lasting contribution to existing knowledge.

TECHNICAL NOTES: Information less broad in scope but nevertheless of importance as a contribution to existing knowledge.

TECHNICAL MEMORANDUMS: Information receiving limited distribution because of preliminary data, security classification, or other reasons.

CONTRACTOR REPORTS: Scientific and technical information generated under a NASA contract or grant and considered an important contribution to existing knowledge.

TECHNICAL TRANSLATIONS: Information published in a foreign language considered to merit NASA distribution in English.

SPECIAL PUBLICATIONS: Information derived from or of value to NASA activities. Publications include conference proceedings, monographs, data compilations, handbooks, sourcebooks, and special bibliographies.

TECHNOLOGY UTILIZATION PUBLICATIONS: Information on technology used by NASA that may be of particular interest in commercial and other non-aerospace applications. Publications include Tech Briefs, Technology Utilization Reports and Notes, and Technology Surveys.

Details on the availability of these publications may be obtained from:

SCIENTIFIC AND TECHNICAL INFORMATION DIVISION
NATIONAL AERONAUTICS AND SPACE ADMINISTRATION
Washington, D.C. 20546